高齢者感染症

高齢者の抗酸菌感染症

Mycobacteriosis in elderly

倉島篤行

Keywords：結核，非結核性抗酸菌症，高齢者，外来性再感染

はじめに

抗酸菌感染症は結核症と非結核性抗酸菌症に二分されるが，疾患の伝染性，有病者数，高齢者における高い罹患率，死亡率などで公衆衛生学的には前者が大きな脅威であることはいうまでもない．

しかし，治療において結核症よりはるかに困難な非結核性抗酸菌症はこの数十年で着実に増加し，近年は毎年の新たな抗酸菌陽性患者の約1/3以上を占めると推定され，我が国の非結核性抗酸菌症罹患率は国際的にも有数の高いレベルと推定され今後大きな課題になると考えられる．

1. 我が国の高齢者結核の特徴

現在，我が国結核の際立った構造的特徴として高齢者が多いということがいえる[1]．2005年の新登録結核28,319人の中で65歳以上が52.8%を占めている．これは我が国人口構成中での高齢者人口そのものの絶対的増加が主因ではあるが，このような結核登録の年齢階級別分布は世界共通なものではなく，我が国，シンガポール，台湾などかつて結核既感染率が非常に高かった国特有の構造である．

図1は日米の2005年での結核罹患実数を同一の年齢階級別区分で表示したものである．米国の人口は我が国の約2.35倍，2005年の結核罹患率は4.8で我が国よりかなり低いが，図のように実数で比較すると規模の大小がよりわかりやすく興味深い図示となる．44歳以下群では日米の新登録結核は，ほぼ同数であるが，45歳以上群では我が国は圧倒的多数ということがわかる．

今日の高齢者は，第二次世界大戦前後の結核罹患率が人口10万対400を超えるような結核高蔓延時代を生き抜いてきたのであり，高い率で結核菌感染を受け，体内に結核菌が潜伏している．

千葉[2]，Southerland[3]らの研究により，結核は感染を受けた人々の生涯を通して約10-20%に発病し，その5-7割は2年以内に集中するが，残りの発病頻度はなだらかなカーブを描いて漸減すると考えられている．長山によるコーホート分析などで示されるように[4]，高齢者の既感染発病はこの減衰カーブの下で発病するのであり，必ずしも高齢による抵抗力の衰えにより既感染発病率が高齢で上昇するわけではない．これに既発病者の再発病を加えた内因性再燃が今日の高齢者の圧倒的多数を占め，絶対数が多いのはこの母集団である高齢者人口の増加によるものである．しかし，近年RFLP分析などから結核の外来性再感染は少なからずあると考えられるようになった．Jasmerらによれば，米国カナダ地域での結核1,075例を母集団とした再発結核75例のRFLP検討結果では，約4%が外来性再感染と考えられたと報告している[5]．再発結核中での外来性再感染率はその地域での結核罹患率に依存する数字であり，恐らく我が国ではその2-3倍の再感染率が推定される．特に高齢者施設内など特殊な環境では更に高いと考えられる．

以上の群のほか，純粋な新規発病群を加えた，複雑な集団から我が国高齢者結核は形成され，高齢者は現代日本の最大の結核ハイリスクグループとなっている．

我が国人口の高齢化は著しく，65歳以上の高齢者は1998年から2,000万人を超え，2040年には3,380万人に達すると推定されている．長山の近未来予測によれば2018年においても，日本では高齢者結核は大きな問題として存続し続けると推定している．

2. 高齢者結核群と他の世代への影響

では高齢者結核群は他の年齢階層への大きな危険因子として影響を及ぼしているだろうか？

井上らは愛知県における1,141人の喀痰塗抹陽性肺結核患者登録から年齢階級別感染源率を解析，報告している[6]．それによれば，感染経路を同じくする複数の発病クラスター中の発端例を感染源とし，二次発病者数に対する割合を感染源率とすると，全年齢では感染源率は6.1%であったが，60歳未満では11.6%，60歳以上では3.3%と有意な差があったとしている．

各種因子についても検討を行っているが，有空洞例が年齢とは独立した感染危険因子であったとしている．従来から高齢者世代から若年者世代への伝搬は想像されるより少ないのではないかということはいわれていたが本報告はそれを裏付けるものであり，著者らはより効率的な高齢者結核対策の提案を行っている．臨床で遭遇する多くの高齢者は，自らが結核高蔓延時代を生き抜いた経歴上，結核伝染に対する自戒の念は現在の中年世代以下群よりはるかに意識的，自制的な場合が多く，一つはこのような自覚に伴う行動様式の反映かもしれない．

3. 高齢者結核臨床像の特徴と問題点

高齢者結核臨床像の特徴として既に多くの報告やメタアナリシス[7]で，合併症数が多く結核死亡率も高い，自覚症に乏しく画像所見でも有空洞型は他の世代群に比べ有意に少ないなどが述べられている．我が国の結核検診では伝統的に胸部X線診断が重視されてきたが，高齢者結

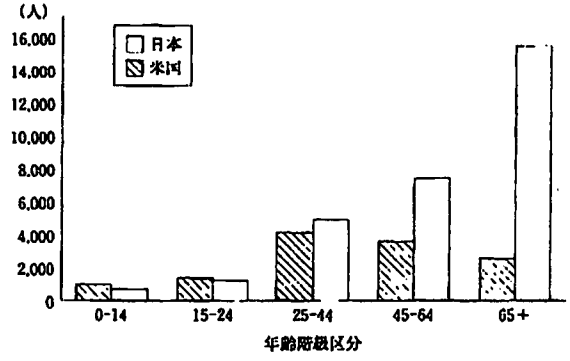

図1　2005年，日米年齢階級区分別新登録結核実数
（結核の統計2006（厚生労働省健康局結核感染症課監修）と米国CDC結核疫学調査報告より作図）

Atsuyuki Kurashima: Division of Clinical Research, National Hospital Organization Tokyo Hospital　独立行政法人国立病院機構東京病院　臨床研究部

0047-1852/07/¥40/頁/JCLS

Available online at www.sciencedirect.com
ScienceDirect
Journal of Microbiological Methods 72 (2008) 149–156
Journal of Microbiological Methods
www.elsevier.com/locate/jmicmeth

Comprehensive analysis of mycolic acid subclass and molecular species composition of *Mycobacterium bovis* BCG Tokyo 172 cell wall skeleton (SMP-105)

Yuko Uenishi [a,*], Yukiko Fujita [b], Naoto Kusunose [c], Ikuya Yano [b], Makoto Sunagawa [d]

[a] *Technology Research & Development Center, Dainippon Sumitomo Pharma Co., Ltd., 1-3-45, Kurakakiuchi, Ibaraki-shi, Osaka 567-0878, Japan*
[b] *Japan BCG Central Laboratory, 3-1-5 Matsuyama, Kiyose-shi, Tokyo 204-0022, Japan*
[c] *Drug Research Division, Dainippon Sumitomo Pharma Co., Ltd., 3-1-98, Kasugade-naka, Konohana-ku, Osaka-shi, Osaka 554-0022, Japan*
[d] *Faculty of Pharmaceutical Sciences, Teikyo Heisei University, 2289-23, Uruido, Ichihara-shi, Chiba 290-0193, Japan*

Received 16 April 2007; received in revised form 21 October 2007; accepted 13 November 2007
Available online 22 November 2007

Abstract

The mycobacterial cell envelope consists of a characteristic cell wall skeleton (CWS), a mycoloyl arabinogalactan peptidoglycan complex, and related hydrophobic components that contribute to the cell surface properties. Since mycolic acids have recently been reported to play crucial roles in host immune response, detailed molecular characterization of mycolic acid subclasses and sub-subclasses of CWS from *Mycobacterium bovis* BCG Tokyo 172 (SMP-105) was performed. Mycolic acids were liberated by alkali hydrolysis from SMP-105, and their methyl esters were separated by silica gel TLC into three subclasses: α-, methoxy-, and keto-mycolates. Each mycolate subclass was further separated by silver nitrate ($AgNO_3$)-coated silica gel TLC into sub-subclasses. Molecular weights of individual mycolic acid were determined by MALDI-TOF mass spectrometry. α-Mycolates were sub-grouped into *cis*, *cis*-dicyclopropanoic (α1), and *cis*-monocyclopropanoic-*cis*-monoenoic (α2) series; methoxy-mycolates were sub-grouped into *cis*-monocyclopropanoic (m1), *trans*-monocyclopropanoic (m2), *trans*-monoenoic (m3), *cis*-monocyclopropanoic-*trans*-monoenoic (m4), *cis*-monoenoic (m5), and *cis*-monocyclopropanoic-*cis*-monoenoic (m6) series; and keto-mycolates were sub-grouped into *cis*-monocyclopropanoic (k1), *trans*-monocyclopropanoic (k2), *trans*-monoenoic (k3), *cis*-monoenoic (k4), and *cis*-monocyclopropanoic-*cis*-monoenoic (k5) series. The position of each functional group, including cyclopropane rings and methoxy and keto groups, was determined by analysis of the meromycolates with fast atom bombardment (FAB) mass spectrometry and FAB mass-mass spectrometry, and the *cis*/*trans* ratio of cyclopropane rings and double bonds were determined by NMR analysis of methyl mycolates. Mycolic acid subclass and molecular species composition of SMP-105 showed characteristic features including newly-identified *cis*-monocyclopropanoic-*trans*-monoenoic mycolic acid (m4).

Keywords: Mycolic acids; BCG-CWS; SMP-105; *M. bovis* BCG Tokyo 172

1. Introduction

The mycobacterial cell envelope consists of numerous high molecular weight lipid components, most of which induce diverse host immune responses (Beckman et al., 1994). The cell wall skeleton (CWS) is unique and ubiquitous; however, the fine structure consisting of mycoloyl arabinogalactan-peptidoglycan complex (McNeil et al., 1991; Brennan and Nikaido, 1995; McNeil, 1999; Brennan, 2003) differs among species of mycobacteria. Recently, CWS of *Mycobacterium bovis* BCG has been reported to be a potent anti-cancer immunotherapeutic, based on the host-anti tumor immune response (Seya et al., 2001; Yoo et al., 2002; Akazawa et al., 2004; Nakajima et al., 2004). However, BCG-CWS is a very large hetero lipoglycan containing mycolic acids, which are very long branched-chain hydroxy fatty acids. The structure-biological activity relationship of BCG-CWS has not been fully established, although analytical studies and anti-tumor therapeutic investigations were started 30 years ago (Azuma et al., 1974; Yamamura et al., 1976a,b; Yasumoto et al., 1976; Nishikawa et al., 1978;

* Corresponding author. Tel.: +81 72 627 8214; fax: +81 72 627 8140.
E-mail address: yuko-uenishi@ds-pharma.co.jp (Y. Uenishi).

0167-7012/$ - see front matter © 2007 Elsevier B.V. All rights reserved.
doi:10.1016/j.mimet.2007.11.016

Yamamura et al., 1979; Yasumoto et al., 1979; Hayashi et al., 1998; Tsuji et al., 2000; Azuma and Seya, 2001; Matsumoto et al., 2001; Begum et al., 2004; Ishii et al., 2005).

Recent studies reported that BCG-CWS shows potent adjuvant activity via Toll-like receptors (TLR)-2 and-4 as a pathogen-associated molecular pattern (PAMP) for host animal immune systems, and both mycolic acids and peptidoglycan moieties play central roles in the expression of such activities in experimental animal systems (Seya et al., 2001; Yoo et al., 2002; Akazawa et al., 2004; Nakajima et al., 2004). Recently, mycolic acids have been reported to be CD-1 restrictive lipid antigens presented by dendritic cells (Beckman et al., 1994), and therefore detailed structure analysis of mycolic acids is required. In the present study, we introduced modern techniques for comprehensive analysis of mycolic acids of BCG-CWS. The structure of each subclass and molecular species of mycolic acids was analyzed on the highly purified CWS from *M. bovis* BCG Tokyo 172 (hereafter called SMP-105) after proteinase digestion, DNAase treatment, and delipidation with organic solvents of crude cell wall preparations. Although cellular mycolic acid composition of *M. bovis* BCG substrains were reported in some detail previously (Minnikin et al., 1984; Kaneda et al., 1986, 1988, 1995; Watanabe et al., 2001, 2002; Fujita et al., 2005a,b), the present paper is the first to describe analytical results of fully-separated mycolic acid subclasses and molecular species of *M. bovis* BCG Tokyo cell wall skeleton (SMP-105).

2. Methods

2.1. Bacterial strain and growth conditions

M. bovis BCG Tokyo 172 was grown at 37 °C on the surface of Sauton medium for 9 days. The bacterial culture was heated at 80 °C for 30 min to inactivate the cells, and then centrifuged.

2.2. Preparation of SMP-105

SMP-105 was prepared from crude cell wall preparation of heat-killed *M. bovis* BCG Tokyo 172, essentially in accordance with a method reported previously (Azuma et al., 1974; Uenishi et al., 2007). Briefly, the heat-inactivated bacterial cells were disrupted with Mini DeBEE (BEE International) at 35 kpsi. The disrupted cells were centrifuged at 6760 ×*g* first to remove large debris and undisrupted cells, and then centrifuged again at 18,000 ×*g* to obtain pellet of whole cell wall (WCW). WCW was incubated with benzonase (Merck) at 25 °C for 17 h, followed by pronase (Sigma-Aldrich) at 37 °C for 17 h to digest nucleic acids and proteins, respectively. The enzyme-digested cell walls were washed with 1% polyoxyethylene (10) octylphenyl ether (Triton X-100), then treated with ethanol, tetrahydrofuran, chloroform, and methanol consecutively to remove lipids, and finally dried to obtain SMP-105.

2.3. Preparation of mycolic acid methyl esters by silica gel TLC

The SMP-105 thus obtained was treated with 0.5 M potassium hydroxide/toluene/ethanol (10:10:1, v/v/v) at 65 °C for 3 h, followed by acidification with diluted hydrochloric acid, and then the mycolic acids were extracted with n-hexane. Crude mycolic acids were methylated with 10% trimethylsilyldiazomethane in *n*-hexane (Nacalai Tesque) for more than 30 min at room temperature. Mycolic acid methyl esters were separated by HPTLC (Silica gel 60, 10 × 10 cm, Merck) and developed with a solvent of n-hexane/ethyl acetate (20:1, v/v) three times. Methyl esters, separated into α-, methoxy-, and keto-mycolates, were extracted from silica gel TLC with chloroform/methanol (4:1, v/v).

2.4. Separation of mycolic acid methyl esters by $AgNO_3$-coated silica gel TLC

Silver nitrate ($AgNO_3$)-coated silica gel plates were prepared for HPTLC (Silica gel 60, 10 × 10 cm, Merck) with a 10% solution of $AgNO_3$ in acetonitrile, followed by drying. Each α-, methoxy-, and keto-mycolate was applied to $AgNO_3$-coated silica gel TLC and separated into two or three spots (described below) with *n*-hexane/ethyl acetate (20:1, v/v) as a solvent system. After visualizing by spraying with water, the sub-subclass mycolic acid methyl esters were recovered from $AgNO_3$-coated silica gel TLC with chloroform and methanol. The amount of each mycolate recovered was determined by weight.

2.5. Mass spectrometric analysis of mycolic acid subclasses

The molecular weight of each mycolic acid methyl ester was determined by MALDI-TOF mass spectrometry on Voyager DE-STR (Applied Biosystems) using 2,5-dihydroxybenzoic acid (2,5-DHB) as a matrix, as reported previously (Laval et al., 2001; Fujita et al., 2005a,b). The positions of cyclopropane rings, and methoxy and keto groups were determined by FAB mass (JEOL JMS-SX102) and FAB mass-mass (JEOL JMS-HX/HX 110A) analyses of methyl meromycolates. The methyl meromycolates were prepared as follows: Mycolic acid methyl ester of each subclass was dissolved in acetone/n-hexane (4:1, v/v) and the hydroxyl group was oxidized with Jones reagent (Bowden et al., 1946; Heilbron et al., 1949) at room temperature for 1 h. The resultant β-keto-ester was extracted with n-hexane. After evaporating the solvent, the residues were dissolved in dehydrated methanol/dehydrated tetrahydrofuran (1:1, v/v) and then treated with sodium methoxide at 50 °C for 3 h. After full methylation, samples were neutralized with 2 M hydrochloric acid, and then extracted with *n*-hexane. The resultant meromycolic acid methyl esters were detected by silica gel TLC, and then extracted with chloroform and methanol. The isolated meromycolic acid methyl esters, having different polar groups in the alkyl chain, were mixed with n-nitrobenzyl alcohol and LiI as a matrix, and applied to FAB mass and FAB mass-mass analyses to determine the positions of the functional groups.

2.6. ^1H NMR analysis of mycolic acid subclasses

^1H NMR (500 MHz) spectra of each mycolic acid subclasses were recorded on a JEOL A-500 spectrometer and chemical shifts were referred to internal $CDCl_3$ (7.24 ppm).

3. Results

3.1. Separation of mycolic acid methyl esters by silica gel TLC

Total mycolic acid methyl esters from SMP-105 were separated into α-, methoxy-, and keto-mycolates by silica gel TLC. The relative amount of each mycolic acid methyl ester subclass recovered from SMP-105 was approximately 17:17:66 w/w/w (Suppl. Fig. 1(a)).

Next, to reveal the detailed molecular species composition, each subclass of mycolic acid methyl ester was further separated by $AgNO_3$-coated silica gel TLC, according to the degree of unsaturation. As a result, α-mycolic acid methyl esters were separated into two major spots (Suppl. Fig. 1(b); spots 2 and 3), and methoxy-and keto-mycolic acid methyl esters were separated into three major spots (Suppl. Fig. 1(b); spots 5, 6, 7 and 9, 10, 11). Each spot was recovered from $AgNO_3$-coated silica gel TLC and subjected to MALDI/TOF mass spectrometry. On $AgNO_3$-coated silica gel TLC, saturated, *trans*-monoenoic and *cis*-monoenoic mycolic acid methyl esters were clearly separated, but separation of *cis*-or *trans*-cyclopropanoic mycolates was unsuccessful. The relative yield of each sub-subclass mycolic acid was as follows: α-mycolate, upper spot 51% and lower spot 3%; methoxy-mycolate, uppermost spot 84%, middle spot 3%, and lowest spot 2%; and keto-mycolate, uppermost spot 78%, middle spot 2% and lowest spot 1%, by weight.

3.2. Identification of mycolic acid methyl ester subclasses and molecular species by MALDI-TOF mass analysis

MALDI-TOF mass spectra of mycolic acid methyl esters from SMP-105 showed major clusters of mass ions due to $[M+Na]^+$ (where M is the molecular mass of the mycolic acid methyl ester sub-subclass). We analyzed each molecular species of methyl mycolate sub-subclass separated by $AgNO_3$-coated silica gel TLC and summarized the MALDI-TOF mass spectrometry data of these mycolic acid types in Table 1.

α-Mycolates are the principal mycolic acid subclass in all mycobacterial species. By $AgNO_3$-coated silica gel TLC, α-mycolic acid methyl esters were further separated into two spots (α1 and α2). Positive MALDI-TOF mass spectra of α1 mycolate from $AgNO_3$-coated silica gel TLC showed distinctively the most abundant mass ion at *m/z* 1173, due to C_{78} α-mycolate with two *cis*-cyclopropane rings (Suppl. Fig. 2(a)). Molecular mass ions due to C_{74}, C_{76}, C_{80}, and C_{82} α-mycolates were also clearly demonstrated. While mass spectra of α2 spot showed the most abundant ion at *m/z* 1159, due to C_{77} α-mycolate with one *cis*-cyclopropane ring and one *cis*-double bond, mass ions due to C_{75}, C_{79}, and C_{81} α-mycolates were also detected (Suppl. Fig. 2(b)). It was revealed that the α1 series of α-mycolates comprised even carbon-numbered mycolates with two *cis*-cyclopropane rings, while the α2 series comprised odd carbon-numbered mycolates with one *cis*-cyclopropane ring and one *cis*-double bond, exclusively. It was also noted that a small but significant amount of ions due to C_{72} (*m/z* 1091), C_{74} (*m/z* 1119), and C_{76} (*m/z* 1147) shorter-chain monoenoic even carbon-numbered α-mycolates were observed in the TOF mass spectrum (Suppl. Fig. 2(b)).

Methoxy-mycolates are a characteristic polar mycolic acid subclass in *M. tuberculosis* complex and *M. bovis* BCG Tokyo 172, but are lacking in some *M. bovis* BCG substrains (Minnikin et al., 1984; Watanabe et al., 2002). The MALDI-TOF mass spectra of uppermost spot of the methoxy-mycolate sub-subclass showed the most abundant ion at *m/z* 1289, due to C_{85} *cis*-monocyclopropanoic methoxy-mycolates, with small amounts of C_{81}, C_{83}, C_{87}, and C_{89} homologues (m1) (Suppl. Fig. 3(a)). This group also contained small amounts of longer-chain even carbon-numbered homologues with centering at C_{84}, C_{86}, and C_{88}, due to *trans*-cyclopropanoic methoxy-mycolate (m2), while the mass spectra of middle spot of the methoxy-mycolate sub-subclass also showed the most abundant ion at *m/*

Table 1
MALDI-TOF mass spectrometry data of mycolic acid sub-subclasses of CWS from *M. bovis* BCG Tokyo 172 (SMP-105)

Mycolic acid type	Sub-sub class	Position on $AgNO_3$ TLC	Total number of carbons in mycolic acid															
			74	75	76	77	78	79	80	81	82	83	84	85	86	87	88	89
α	α1	2	1117		1145		**1173**		1201		1229							
	α2	3		**1131**		**1159**		**1187**		1215								
Methoxy	m1	5								1233		**1261**		**1289**		**1317**		1345
	m2												1275		1303		1331	
	m3	6								1233		**1261**		**1289**		1317		
	m4								1217		1245		1273		1301		1329	
	m5	7								1233	1247	1261	**1275**	1289	1303		1331	1345
	m6											1259		1287		1315		1343
Keto	k1	9							1217		**1245**		**1273**		**1301**		1329	
	k2											1259		1287		**1315**		1343
	k3	10							1217		**1245**		**1273**		1301			
	k4	11						1203		**1231**		**1259**		1287		1315		
	k5												1271		1299		1327	

Values represent the pseudomolecular mass $[M+Na]^+$ of methyl mycolate. Subtypes of mycolic acids are α1, *cis*, *cis*-dicyclopropanoic; α2, *cis*-monocyclopropanoic-*cis*-monoenoic; m1, *cis*-monocyclopropanoic methoxy; m2, *trans*-monocyclopropanoic methoxy; m3, *trans*-monoenoic methoxy; m4, *cis*-monocyclopropanoic-*trans*-monoenoic methoxy; m5, *cis*-monoenoic methoxy; m6, *cis*-monocyclopropanoic-*cis*-monoenoic methoxy; k1, *cis*-monocyclopropanoic keto; k2, *trans*-monocyclopropanoic keto; k3, *trans*-monoenoic keto; k4, *cis*-monoenoic keto; and k5, *cis*-monocyclopropanoic-*cis*-monoenoic keto mycolic acids. Major homologues are shown in bold.

z 1289, due to C_{85} monoenoic methoxy-mycolate, with smaller amounts of C_{81}, C_{83}, and C_{87} homologues (m3) (Suppl. Fig. 3 (b)). Furthermore, in this subgroup, small but significant amounts of ions due to even carbon-numbered diene-equivalent methoxy-mycolates were observed, centering at C_{84} and ranging from C_{80} to C_{88} (m4). Judging from the chromatographic behaviors and mass numbers, the former (m3) should be *trans*-monoenoic methoxy-mycolate exclusively, while the latter (m4) should be *cis*-monocyclopropanoic-*trans*-monoenoic methoxy-mycolate, as yet not reported in *M. bovis* BCG. The mass spectra of lowest spot of the methoxy-mycolate sub-subclass showed the most abundant ion at *m/z* 1275, due to C_{84} *cis*-monoenoic methoxy-mycolate, with smaller amounts of C_{81} to C_{89} homologues (m5) (Suppl. Fig. 3(c)). Furthermore, also in this subgroup, small but significant amounts of ions due to odd carbon-numbered diene-equivalent methoxy-mycolates were observed, centering at C_{87} and ranging from C_{83} to C_{89} (m6). Judging from the chromatographic behaviors and mass numbers, the former (m5) should be *cis*-monoenoic methoxy-mycolate, while the latter (m6) should be *cis*-monocyclopropanoic-*cis*-monoenoic methoxy-mycolate, exclusively.

Keto-mycolates are another of the major mycolate subclasses, distributed widely among rapid-and slow-growing mycobacteria. The MALDI-TOF mass spectra of uppermost spot of the keto-mycolate sub-subclass showed the most abundant ion at *m/z* 1273, due to C_{84} monocyclopropanoic keto-mycolate, with smaller amounts of C_{80}, C_{82}, C_{86}, and C_{88} even carbon-numbered homologues (k1) (Suppl. Fig. 4(a)). Furthermore, in this series, substantial amounts of ions due to longer chain odd carbon-numbered monoene-equivalent keto-mycolates were observed, centering at C_{87} and ranging from C_{83} to C_{89} (k2). Judging from the chromatographic behaviors and mass numbers, the former (k1) should be *cis*-monocyclopropanoic keto-mycolates, while the latter (k2) should be *trans*-monocyclopropanoic keto-mycolates, exclusively. The mass spectra of middle spot of the keto-mycolate sub-subclass also showed the most abundant ion at *m/z* 1273, due to C_{84} monoenoic keto-mycolate with smaller amounts of C_{80}, C_{82}, and C_{86} homologues (k3) (Suppl. Fig. 4(b)). Based on the chromatographic behaviors, k3 possesses one *trans*-double bond, exclusively. The mass spectra of lowest spot of the keto-mycolate sub-subclass showed the most abundant ion at *m/z* 1259, due to C_{83} monoenoic keto-mycolate with smaller amounts of C_{79}, C_{81}, C_{85}, and C_{87} homologues (k4) (Suppl. Fig. 4(c)). Furthermore, also in this sub-subgroup, small but significant amounts of ions due to longer chain even carbon-numbered diene equivalent keto-mycolates were observed, centering at C_{86} and ranging from C_{84} to C_{88} (k5). Judging from the chromatographic behaviors and mass numbers, the former (k4) should be *cis*-monoenoic keto-mycolates, while the latter (k5) should be *cis*-monocyclopropanoic-*cis*-monoenoic keto-mycolates.

3.3. Determination of the location of functional groups of mycolic acid sub-subclasses by FAB mass-mass analysis

To determine the locations of the functional groups of mycolic acids from SMP-105, meromycolic acid methyl esters were prepared and analyzed by FAB mass-mass analysis. Methyl meromycolates were prepared by a facile method, different from the pyrolysis reported by Watanabe et al. (2002): Jones oxidation of each methyl mycolate and the following retro-Dieckmann reaction yielded the desired methyl meromycolates (Suppl. Fig. 5). In the present study, the locations of *cis*- and *trans*-double bonds, *cis*-and *trans*-cyclopropane rings, methoxy and keto groups, and methyl branches adjacent to the methoxy or keto groups were determined based on the characteristic bond-cleavage profiles (Tomer et al., 1986; Cheng and Gross, 1998). Functional groups nearer to the carboxyl group are referred to as "proximal," whereas the others are referred to as "distal," for convenience.

FAB mass spectra of α-meromycolates from upper spot showed one major and one minor peak due to the molecular ions at *m/z* 777 and 805, respectively. A mass ion at *m/z* 777, corresponding to the meromycolate derived from C_{78} α-mycolate with two *cis*-cyclopropane rings (α1), the most abundant α-mycolate species, was further decomposed by FAB mass-mass spectroscopy, and the prominent ions due to cleavages at the β-position of the distal and proximal cyclopropane rings were detected (Suppl. Fig. 6(a)). As a result, the position of the distal cyclopropane ring of C_{52} α-meromycolate derived from C_{78} *cis*, *cis*-dicyclopropanoic α-mycolate was shown to be located at the 21st position from the omega end of the alkyl chain, while that of the proximal ring was considered to be at the 13th position from the carboxyl end, exclusively. Similarly, in the case of other dicyclopropanoyl α-mycolates, the distal *cis*-cyclopropane ring was consistently located at the 21st position from the omega end of the meromycolate chain, while the location of the proximal ring was variable according to the chain length of meromycolates. The location of the *cis*-, but not *trans*-double bond, of monocyclopropanoic monoenoic α-mycolate sub-subclass (α2) is most likely identical to those of the corresponding di-*cis*-cyclopropane rings. Most of the analytical data obtained above agreed with those reported previously (Watanabe et al., 2002), although quantitative results differed.

FAB mass spectra of methoxy-meromycolates from upper spot showed five or more peaks due to multi sub-subclasses and molecular species, among which ions at *m/z* 865, 893, and 921 were further decomposed by FAB mass-mass spectroscopy. The mass-mass spectrum of the ion at 893, due to C_{59} methoxy-meromycolate derived from C_{85} methoxy-mycolate with a monocyclopropane ring, mono methyl branch, and methoxy function (m1) (Suppl. Fig. 6(b)). The results showed a characteristic ion at *m/z* 597, due to the cleavage between each pair of carbon units having a methyl branch and methoxy function, and the loss of the methyl group from the latter. With the ion at *m/z* 609, due to the α-cleavage to methyl branch and the loss of the O-methyl group, the location of the methyl branch was identified to be at the 19th position from the omega end, and that of the adjacent methoxy group was judged to be at the 20th position, exclusively. Furthermore, since this molecular species was suggested to possess one cyclopropane ring at the proximal position, the location was again identified based on the β-cleavage at both sides of the ring. The results showed prominent ions at *m/z* 289 and 357, indicating the *cis*-cyclopropane ring was located at the 19th position from the

carboxyl end of the meromycolate. The locations of the functional groups of meromycolates belonging to other series were determined similarly. The locations of the methyl branch and O-methyl groups from the omega end of meromycolates were essentially the same among all the methoxy-mycolic acid sub-subclasses, while those of other proximal functional groups such as *cis*-or *trans*-cyclopropane rings, or *cis*-and *trans*-double bonds differed according to the chain length of the meromycolate, reflecting the biosynthetic mechanism and introduction rule of functional groups into meromycolic acids. It was particularly noted that the methoxy-mycolic acid sub-subclass was composed mainly of odd carbon-numbered *trans*-monoenoic methoxy-mycolate (m3), and further, the same methoxy-mycolate subclass showed substantial intensity of mass ions due to even carbon-numbered diene-equivalent subspecies (m4), centering at C_{84} and ranging from C_{80} to C_{88}. Although such diene-equivalent series of even carbon-numbered methoxy-mycolates has not been reported in *M. bovis* BCG substrains, these molecular species or subclasses seemed most likely to be *cis*-monocyclopropanoic-*trans*-monoenoic methoxy-meromycolates. These results were confirmed by NMR analysis.

FAB mass spectra of keto-meromycolates from upper spot showed ten or more peaks due to diverse subclasses and molecular species composition, among which ions at *m/z* 877, 905, and 919 were further decomposed by FAB mass-mass spectroscopy. The mass-mass spectrum of the ion at 877, due to C_{58} keto-meromycolic acid derived from C_{84} keto-mycolate (k1) with a monocyclopropane ring, monomethyl branch, and carbonyl functions (Suppl. Fig. 6(c)). The results showed characteristic ions at *m/z* 553 and 637, due to the β-cleavages of both sides of two functional groups ($-CH_2-CO-CH(CH_3)-CH_2-$). These fragmentations indicate the existence of a methyl group and an adjacent carbonyl group at the 19th position from the omega end, and therefore the 37th position of the carboxy end of meromycolate, exclusively. Furthermore, since this molecular species was suggested to possess one cyclopropane ring at the proximal position, the location was again identified based on the β-cleavage at both sides of the ring. The results showed the ions at *m/z* 289 and 357, indicating the proximal *cis*-cyclopropane ring was probably located at the 19th position from the carboxyl end of the meromycolate. The locations of the functional groups of keto-meromycolates belonging to other series were determined similarly.

3.4. ^1H NMR analysis of mycolic acid subclasses

^1H NMR spectra of α-, methoxy-, and keto-mycolates, each major spot obtained by $AgNO_3$-coated silica gel TLC, were recorded and shift values were measured in ppm (δ) relative to internal $CHCl_3$. An ^1H NMR spectrum (Suppl. Fig. 7(a)) of the most abundant subclass α1-mycolates with two cyclopropane rings, showing common signals of mycolic acid methyl esters, such as those due to $-(CH_2)_nCH_3$,$-CH_2(CH_2)_nCH_2-$,$-CH_2CH(OH)-$,$-CH_2CH(COOCH_3)-$,$-CH(COOCH_3)-$,$-CH(OH)-$, and $-COOCH_3$, as well as α1 subclass-specific signals, such as those due to *cis*-cyclopropane rings at around δ 0.53 to 0.62 and δ −0.36. An ^1H NMR spectrum (Suppl. Fig. 7(b)) of the most abundant subclass methoxy-mycolates including m1 and m2 with one *cis*-or *trans*-cyclopropane ring, showing methoxy-mycolic acid methyl ester-specific signals, such as those due to $-CHOCH_3$ at δ 3.30 with a *cis*-cyclopropane ring. An ^1H NMR spectrum (Suppl. Fig. 7(c)) of the most abundant keto-subclass mycolates including k1 and k2 with one cyclopropane ring including both *cis*-and *trans*-configurations. All ^1H NMR parameters for each of these mycolic acid subclasses are listed in Table 2. Based on the combined results obtained from mass spectrometric analyses (MALDI-TOF mass and FAB mass) and ^1H NMR parameters, it was concluded that α-mycolates (α1 and α2) contained one or two *cis*-cyclopropane ring(s) but did not contain *trans*-cyclopropane rings; methoxy-mycolates (m1 and m2) contained one cyclopropane ring with *cis*-or *trans*-configurations in which the *cis*-form predominated; and keto-mycolates (k1 and k2) also contained one cyclopropane ring with *cis*-or *trans*-configurations in which the *cis*-form predominated, but more *trans*-form existed than in the case of methoxy-mycolates. The *cis*-to *trans*-form ratios in methoxy- and keto-mycolates were calculated using the accumulated

Table 2
^1H NMR signals characteristic of methyl mycolate subclasses of CWS from *M. bovis* BCG Tokyo 172 (SMP-105)

Mycolic acid type	Sub-sub class	Position on $AgNO_3$ TLC	Δ	$-CHCH_3$	$-CHOR$	$-CHOCH_3$	*cis*/trans
α	α1	2	−0.36 (m, 1H) cis 0.53 (m, 1H) cis 0.62 (m, 2H) cis				100:0
Methoxy	m1 and m2	5	−0.36 (m, 1H) cis 0.53 (m, 1H) cis 0.62 (m, 2H) cis 0.04 to 0.19 (m, 3H) trans 0.42 (m, 1H) trans	0.85 (d, 3H)	2.93 (m, 1H)	3.30 (s, 3H)	91:9
Keto	k1 and k2	9	−0.36 (m, 1H) cis 0.53 (m, 1H) cis 0.62 (m, 2H) cis 0.04 to 0.19 (m, 3H) trans 0.42 (m, 1H) trans	0.85 (d, 3H)	–	–	71:29

Common signals to all mycolic acid methyl esters: δ 0.86 ($-(CH_2)_nCH_3$, t, 6H), δ 1.0–1.5 ($-CH_2(CH_2)_nCH_2-$, br, m), δ 1.54 ($-CH_2CH(OH)-$, m, 2H), δ 1.66 ($-CH_2CH(CO_2CH_3)-$, m, 2H), δ 2.40 ($-CH(CO_2CH_3)-$, m, 1H), δ 3.62 ($-CH(OH)-$, br, m, 1H), δ 3.68 ($(-CO_2CH_3)-$, s, 3H).
br; broad, s; singlet, d; doublet, t; triplet, m; multiplet.

intensity of peaks attributable to the *cis*-form observed at around δ 0.53 to 0.62 and δ −0.36, and that of peaks attributable to *trans*-form at around δ 0.42 and δ 0.04 to 0.19. As a result, it was concluded that the ratio of *cis*- to *trans*-form of cyclopropane rings of methoxy-mycolates (m1 and m2) was 91:9 and that of keto-mycolates (k1 and k2) was 71:29.

As described above, among the three subclasses of mycolic acids, six sub-subclasses of methoxy-mycolates were specific to

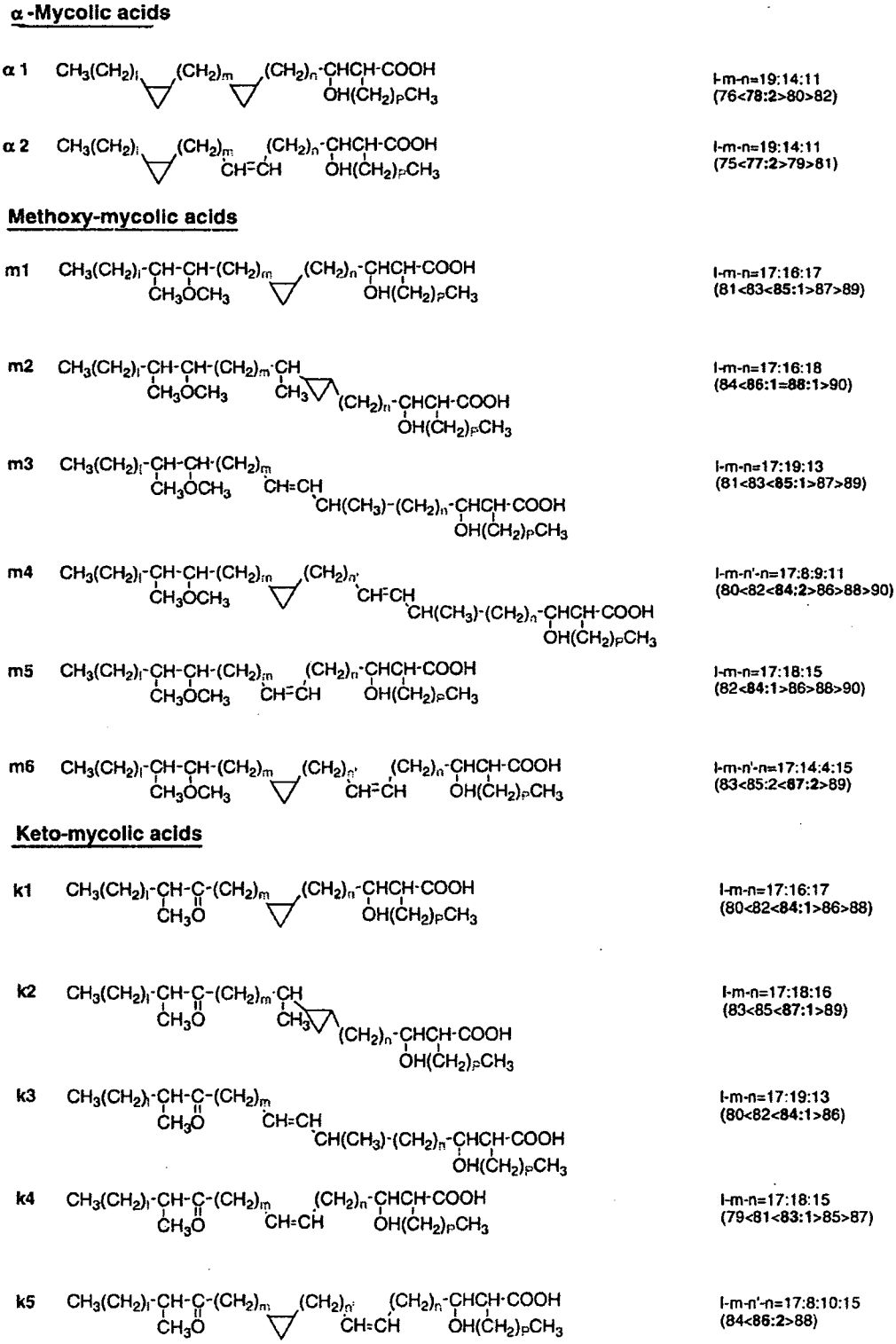

Fig. 1. Structures of 13 subclasses of mycolic acids of CWS from *M. bovis* BCG Tokyo 172 (SMP-105).

SMP-105. In addition, the fact that the ratio of *cis*-to *trans*-form in α-, methoxy-, and keto-mycolates increased in the order 100:0, 91:9, and 71:29 was considered to be another unique characteristic of SMP-105.

Fig. 1 summarizes the possible structures of the thirteen types of mycolic acids separated from SMP-105, based on the chromatographic behaviors, MALDI-TOF and FAB mass analyses, NMR analysis and on deduction based on findings from previous reports (Watanabe et al., 2001, 2002).

4. Discussion

Mycolic acids are the most characteristic high molecular weight bioactive lipid component of the mycobacterial cell envelope, and their structures vary greatly according to mycobacterial species, culture conditions, and lipid classes (Minnikin et al., 1984; Kaneda et al., 1986, 1988, 1995; Watanabe et al., 2001, 2002; Fujita et al., 2005a,b; Fujita et al., 2007). As it has been reported that subclass composition of mycolic acids differs among *M. bovis* BCG substrains after multiple passages (Behr et al., 2002), we carefully separated total mycolic acid methyl esters of CWS derived from *M. bovis* BCG Tokyo 172 (SMP-105) by silica gel TLC. As a result, it was clearly demonstrated that three subclasses and thirteen sub-subclasses of mycolic acid methyl esters, including α-, methoxy-and keto-mycolates exist. The separation was satisfactory and this pattern differed from that of *M. bovis* BCG Pasteur or Connaught strains, which possess only α-and keto-mycolic acids. Since the wild strain of *M. bovis* B-10 contains α-, methoxy-and keto-mycolic acids in a ratio of roughly 1:2:1 by weight, the existence of methoxy-mycolates may affect the morphology and immunopotentiating activities of mycoloyl glycolipids, and BCG-CWS may have distinctive immunomodulatory activities (Azuma et al., 1974; Hayashi et al., 1998; Azuma and Seya, 2001). Sub-subclass analysis of α-, methoxy-, and keto-mycolates in SMP-105 was first performed by $AgNO_3$-coated silica gel TLC, which allowed the separation of methyl mycolates into saturated, *cis*-and *trans*-monoenoic, and *cis*-and *trans*-dienoic mycolic acid sub-subclasses. Each spot on $AgNO_3$-coated silica gel TLC was recovered and analyzed by MALDI/TOF and FAB mass spectrometry and NMR. As a result, α-mycolates were separated into *cis*, *cis*-dicyclopropanoic acids centering at C_{78} (α1), and *cis*-monocyclopropanoic-*cis*-monoenoic acids centering at C_{77} (α2). Methoxy-mycolates were grouped into six subclasses: *cis*-monocyclopropanoic acids centering at C_{85} (m1), smaller amounts of *trans*-monocyclopropanoic acids centering at C_{86} and C_{88} (m2), *trans*-monoenoic acids centering at C_{85} (m3), a novel series of *cis*-monocyclopropanoic-*trans*-monoenoic acids centering at C_{84} (diene-equivalent) (m4), *cis*-monoenoic acids centering at C_{84} (m5), and *cis*-monocyclopropanoic-*cis*-monoenoic acids centering at C_{87} (m6). Keto-mycolates were grouped into five subclasses: *cis*-monocyclopropanoic acids centering at C_{84} (k1), a substantial amount of *trans*-monocyclopropanoic acids centering at C_{87} (k2), *trans*-monoenoic acids centering at C_{84} (k3), *cis*-monoenoic acids centering at C_{83} (k4), and *cis*-monocyclopropanoic-*cis*-monoenoic acids centering at C_{86} (diene-equivalent) (k5). Although structure analysis of subclass or molecular species composition of the cellular mycolic acids of *M. bovis* BCG substrains have already been reported (Minnikin et al., 1984; Kaneda et al., 1986, 1988, 1995; Watanabe et al., 2001, 2002), the present report is the first describing the detailed analytical study of the mycolic acid subclass and molecular species composition of SMP-105. Particularly interesting is the existence of six sub-subclasses of methoxy-mycolic acid, and of novel *cis*-monocyclopropanoic-*trans*-monoenoic methoxy-mycolic acid (m4), all of which are entirely lacking in the recently mutated BCG substrains that have appeared after the mma-3 mutation in 1927 (Behr et al., 2000; Belly et al., 2004).Thus, sub-subclass separation and identification of mycolic acids in mycobacterial lipids revealed new information on particular mycolic acid molecules. Recently, we have demonstrated that *M. leprae* cord factor (TDM) contained α-and only one sub-subclass *cis*-monoenoic keto-mycolic acid with 81 or 83 carbon atoms (Kai et al., 2007), although the subclass composition was the same as that of *M. bovis* BCG. On the other hand, as deduced from NMR analysis, the *cis*/*trans*-ratio of the mycolic acid subclass decreased in the order of α->methoxy-> keto-mycolates. Since recent studies have shown that *trans*-cyclopropanation of mycolic acids suppresses *M. tuberculosis*-induced inflammation and virulence (Yuan et al., 1998; Rao et al., 2006), the structure-biological activity relationship should be investigated more precisely. Taken together, presence of keto-mycolic acid, but absence of methoxy-mycolate may affect toxicity, immunogenicity and intracellular persistency in host animals. Although BCG daughter strains have been attenuated over the 80 years that have elapsed since initial passage and their immunological properties have changed, the cell wall skeleton of *M. bovis* BCG Tokyo 172, an early strain of BCG vaccine, still shows potent immunostimulatory activities, and mycolic acids seem to play critical roles. In the near future, comparative studies on the mycolic acid structures and immunopotential activity relationships among mycobacterial species should be established.

Acknowledgements

We thank Tomoko Sugiyama for her technical assistance and Francis Cinget for NMR analysis.

Appendix A. Supplementary data

Supplementary data associated with this article can be found, in the online version, at doi:10.1016/j.mimet.2007.11.016.

References

Akazawa, T., Masuda, H., Saeki, Y., Matsumoto, M., Takeda, K., Tsujimura, K., Kuzushima, K., Takahashi, T., Azuma, I., Akira, S., Toyoshima, K., Seya, T., 2004. Adjuvant-mediated tumor regression and tumor-specific cytotoxic response are impaired in MyD88-defficient mice. Cancer Res. 64, 757–764.

Azuma, I., Seya, T., 2001. Development of immunoadjuvants for immunotherapy of cancer. Int. Immunopharmacol. 1, 1249–1259.

Azuma, I., Ribi, E.E., Meyer, T.J., Zbar, B., 1974. Biologically active components from mycobacterial cell walls. I. Isolation and composition of cell wall skeleton and components P_3. J. Natl. Cancer Inst. 52, 95–101.

Beckman, E.M., Porcelli, S.A., Morita, C.T., Behar, S.M., Furlong, S.T., Brenner, M.B., 1994. Recognition of a lipid antigen by CD1-restricted alpha beta+ T cells. Nature 372, 691–694.

Begum, N.A., Ishii, K., Kurita-Taniguchi, M., Tanabe, M., Kobayashi, M., Moriwaki, Y., Matsumoto, M., Fukumori, Y., Azuma, I., Toyoshima, K., Seya, T., 2004. *Mycobacterium bovis* BCG cell-wall specific differentially expressed genes identified by differential display and cDNA subtraction in human macrophages. Infect. Immun. 72, 937–948.

Behr, M.A., Schroeder, B.G., Brinkman, J.N., Slayden, R.A., Barry III, C.E., 2000. A point mutation in the mma3 gene is responsible for impaired methoxymycolic acid production in *Mycobacterium bovis* BCG strains obtained after 1927. J. Bacteriol. 182, 3394–3398.

Belly, A., Alexander, D., Di Pietrantonio, T., Girard, M., Jones, J., Schurr, E., Liu, J., Sherman, D.R., Behr, M.A., 2004. Impact of methoxymycolic acid production by *Mycobacterium bovis* BCG strains. Infect. Immun. 72, 2803–2809.

Bowden, K., Heilbron, I.M., Jones, E.R.H., Weedon, B.C.L., 1946. Researches on acetylenic compounds. Part I. The preparation of acetylenic ketones by oxidation of acetylenic carbinols and glycols. J. Chem. Soc. 39–45.

Brennan, P.J., 2003. Structure, function, and biogenesis of the cell wall of *Mycobacterium tuberculosis*. Tuberculosis 83, 91–97.

Brennan, P.J., Nikaido, H., 1995. The envelope of mycobacteria. Annu. Rev. Biochem. 64, 29–63.

Cheng, C., Gross, M.L., 1998. Fragmentation mechanisms of oxofatty acids via high-energy collisional activation. J. Am. Soc. Mass Spectrom. 9, 620–627.

Hayashi, A., Doi, O., Azuma, I., Toyoshima, K., 1998. Immuno-friendly use of BCG-cell wall skeleton remarkably improves the survival rate of various cancer patients. Proc. Jpn. Acad. 74, 50–55.

Heilbron, I.M., Jones, E.R.H., Sondheimer, F., 1949. Research on acetylenic compounds. Part XV. The oxidation of primary acetylenic carbinols and glycols. J. Chem. Soc. 604–607.

Fujita, Y., Naka, T., Doi, T., Yano, I., 2005a. Direct molecular mass determination of trehalose monomycolate from 11 species of mycobacteria by MALDI-TOF mass spectrometry. Microbiology 151, 1443–1452.

Fujita, Y., Naka, T., McNeil, M.R., Yano, I., 2005b. Intact molecular characterization of cord factor (trehalose 6,6'-dimycolate) from nine species of mycobacteria by MALDI-TOF mass spectrometry. Microbiology 151, 3403–3416.

Fujita, Y., Okamoto, Y., Uenishi, Y., Sunagawa, M., Uchiyama, T., Yano, I., 2007. Molecular and supra-molecular structure related differences in toxicity and granulomatogenic activity of mycobacterial cord factor in mice. Microb. Pathog. 43, 10–21.

Ishii, K., Kurita-Taniguchi, M., Aoki, M., Kimura, T., Kahiwazaki, Y., Matsumoto, M., Seya, T., 2005. Gene-inducing program of human dendritic cells in response to BCG CWS, which reflects adjuvancy required for tumor immunotherapy. Immunol. Lett. 98, 280–290.

Kai, M., Fujita, Y., Maeda, Y., Nakata, N., Izumi, S., Yano, I., Makino, M., 2007. Identification of trehalose dimycolate (cord factor) in *Mycobacterium leprae*. FEBS Lett. 581, 3345–3350.

Laval, F., Laneelle, M.A., Deon, C., Monsarrat, B., Daffe, M., 2001. Accurate molecular mass determination of mycolic acids by MALDI-TOF mass spectrometry. Anal. Chem. 73, 4537–4544.

Matsumoto, M., Seya, T., Kikkawa, S., Tsuji, S., Shida, K., Nomura, M., Kurita-Taniguchi, M., Ohigashi, H., Yokouchi, H., Takami, K., Hayashi, A., Azuma, I., Masaoka, T., Kodama, K., Toyoshima, K., Higashiyama, M., 2001. Interferon gamma-producing ability in blood lymphocytes of patients with lung cancer through activation of the innate immune system by BCG cell wall skeleton. Int. Immunopharmacol. 1, 1559–1569.

McNeil, M.R., 1999. Arabinogalactan in mycobacteria: structure, biosynthesis and genetics. In: Goldberg, Joanna B. (Ed.), Genetics of Bacterial Polysaccharides. CRC Press, Boca Raton, FL, pp. 207–223.

McNeil, M.R., Daffe, M., Brennan, P.J., 1991. Location of the mycolyl ester substituents in the cell walls of mycobacteria. J. Biol. Chem. 266, 13217–13223.

Minnikin, D.E., Parlett, J.H., Magnusson, M., Ridell, M., Lind, A., 1984. Mycolic acid patterns of representatives of *Mycobacterium bovis* BCG. J. Gen. Microbiol. 130, 2733–2736.

Nakajima, H., Kawasaki, K., Oka, Y., Tsuboi, A., Kawakami, M., Ikegami, K., Hoshida, Y., Fujiki, F., Nakano, A., Masuda, T., Wu, F., Taniguchi, Y., Yoshihara, S., Elisseeva, O.A., Oji, Y., Ogawa, H., Azuma, I., Kawase, I., Aozasa, K., Sugiyama, H., 2004. WT1 peptide vaccination combined with BCG-CWS is more efficient for tumor eradication than WT1 peptide vaccination alone. Cancer Immunol. Immunother. 53, 617–624.

Nishikawa, H., Yasaki, S., Yoshimoto, T., Sakatani, M., Itoh, M., Masuno, T., Namba, M., Ogura, T., Hirao, F., Azuma, I., Yamamura, Y., 1978. Effect of BCG cell-wall skeleton immunotherapy on the peripheral blood lymphocytes in patients with lung cancer after radiotherapy. Gann 69, 819–824.

Kaneda, K., Naito, S., Imaizumi, S., Yano, I., Mizuno, S., Tomiyasu, I., Baba, T., Kusunose, E., Kusunose, M., 1986. Determination of molecular species composition of C_{80} or longer-chain α-mycolic acids in *Mycobacterium* spp. by gas chromatography-mass spectrometry and mass chromatography. J. Clin. Microbiol. 24, 1060–1070.

Kaneda, K., Imaizumi, S., Mizuno, S., Baba, T., Tsukamura, M., Yano, I., 1988. Structure and molecular species composition of three homologues series of α-mycolic acids from *Mycobacterium* spp. J. Gen. Microbiol. 134, 2213–2229.

Kaneda, K., Imaizumi, S., Yano, I., 1995. Distribution of C_{22}-, C_{24}-and C_{26}-α-unit-containing mycolic acid homologues in mycobacteria. Microbiol. Immunol. 39, 563–570.

Rao, V., Gao, F., Chen, B., Jacobs Jr., W.R., Glickman, M.S., 2006. *Trans*-cyclopropanation of mycolic acids of trehalose dimycolate suppresses *Mycobacterium tuberculosis*-induced inflammation and virulence. J. Clin. Invest. 116, 1660–1667.

Seya, T., Matsumoto, M., Tsuji, S., Begum, N.A., Nomura, M., Azuma, I., Hayashi, A., Toyoshima, K., 2001. Two receptor theory in innate immune activation: studies on the receptors for bacillus Calmette Guerin-cell wall skeleton. Arch. Immunol. Ther. Exp. 49 (Suppl. 1), S13–S21.

Tomer, K.B., Jensen, N.J., Gross, M.L., 1986. Fast atom bombardment and tandem mass spectrometry for determining structural modification of fatty acids. Anal. Chem. 58, 2429–2433.

Tsuji, S., Matsumoto, M., Takeuchi, O., Akira, S., Azuma, I., Hayashi, A., Toyoshima, K., Seya, T., 2000. Maturation of human dendritic cells by cell wall skeleton of *Mycobacterium bovis* bacillus Calmette-Guerin: involvement of toll-like receptors. Infect. Immun. 68, 6883–6890.

Uenishi, Y., Okada, T., Okabe, S., Sunagawa, M., 2007. Study on the cell wall skeleton derived from *Mycobacterium bovis* BCG Tokyo 172 (SMP-105): establishment of preparation and analytical methods. Chem. Pharm. Bull. 55, 843–852.

Watanabe, M., Aoyagi, Y., Ridell, M., Minnikin, D.E., 2001. Separation and characterization of individual mycolic acids in representative mycobacteria. Microbiology 147, 1825–1837.

Watanabe, M., Aoyagi, Y., Mitome, H., Fujita, T., Naoki, H., Ridell, M., Minnikin, D.E., 2002. Location of functional groups in mycobacterial meromycolate chains; the recognition of new structural principles in mycolic acids. Microbiology 148, 1881–1902.

Yamamura, Y., Azuma, I., Taniyama, T., Sugimura, K., Hirao, F., Tokuzen, R., Okabe, M., Nakahara, W., Yasumoto, K., Ohta, M., 1976a. Immunotherapy of cancer with cell wall skeleton of *Mycobacterium bovis*-Bacillus Calmette-Guerin: experimental and clinical results. Ann. N.Y. Acad. Sci. 277, 209–227.

Yamamura, Y., Ogura, T., Yoshimoto, T., Nishikawa, H., Sakatani, M., 1976b. Successful treatment of the patients with malignant pleural effusion with BCG cell-wall skeleton. Gann 67, 669–677.

Yamamura, Y., Sakatani, M., Ogura, T., Azuma, I., 1979. Adjuvant immunotherapy of lung cancer with BCG cell-wall skeleton (BCG-CWS). Cancer 43, 1314–1319.

Yasumoto, K., Manabe, H., Ueno, M., Ohta, M., Ueda, H., 1976. Immunotherapy of human lung cancer with BCG cell-wall skeleton. Gann 67, 787–795.

Yasumoto, K., Manabe, H., Yanagawa, E., Nagano, N., Ueda, H., Hirota, N., Ohta, M., Nomoto, K., Azuma, I., Yamamura, Y., 1979. Nonspecific adjuvant immunotherapy of lung cancer with cell wall skeleton of *Mycobacterium bovis* Bacillus Calmette-Guerin. Cancer Res. 39, 3262–3267.

Yoo, Y.C., Hata, K., Lee, K.B., Azuma, I., 2002. Inhibitory effect of BCG cell-wall skeletons (BCG-CWS) emulsified in squalane on tumor growth and metastasis in mice. Arch. Pharm. Res. 25, 522–527.

Yuan, Y., Zhu, Y., Crane, D.D., Barry III, C.E., 1998. The effect of oxygenated mycolic acid composition on cell wall function and macrophage growth in *Mycobacterium tuberculosis*. Mol. Microbiol. 29, 1449–1458.